International Journal of Nanomedicine

Dovepress
Taylor & Francis Group

Open Access Full Text Article

ORIGINAL RESEARCH

Heme Oxygenase-1 Modulates Macrophage Polarization Through Endothelial Exosomal miR-184-3p and Reduces Sepsis-Induce Lung Injury

Wei Chen[1,*], Yuan Zhang[1–3,*], Jinkun Chen[1,*], Shuan Dong[1–3], Xiaoyang Wu[1], Ya Wu[1], Zhuo Du[1], Yibo Yang[1], Lirong Gong[1–3], Jianbo Yu[1–3]

[1]Tianjin Nankai Hospital, Tianjin Medical University, Tianjin, 300100, People's Republic of China; [2]Institute of Integrative Medicine for Acute Abdominal Diseases, Tianjin, 300100, People's Republic of China; [3]Tianjin Key Laboratory of Acute Abdomen Disease Associated Organ Injury and ITCWM Repair, Tianjin, 300100, People's Republic of China

*These authors contributed equally to this work

Correspondence: Jianbo Yu; Lirong Gong, Tianjin Nankai Hospital, Tianjin Medical University, 6 Changjiang Road, Nankai District, Tianjin, 300100, People's Republic of China, Email 30717008@nankai.edu.cn; soundglr@163.com

Introduction: Pulmonary microvascular endothelial cells (PMVECs) are notably implicated in the pathogenesis of sepsis-induced lung injury. Exosomes derived from PMVECs facilitate intercellular communication among various cell types, especially crosstalk with macrophages. Heme oxygenase-1 (HO-1), an early stress-responsive enzyme with inherent protective functions, has been implicated in acute lung injury (ALI) mitigation. But research on the mechanism of HO-1 in macrophage polarization via PMVEC exosomes in sepsis-induced lung injury is lacking.

Methods: To investigate the role of HO-1 in the interaction between endothelial cells and macrophages, HO-1 knockout mouse model were established. Exosomes from PMVECs were isolated, and differential expression of microRNA (miRNA) was determined by sequencing. An in vitro co-culture system involving Murine Alveolar Macrophage Cell Line (MH-S cells) and HO-1/ PMVECs-derived exosomes (HP-exos) was used to investigate the underlying mechanisms. To further verify the involvement of HO-1 in intercellular communication through exosomal miRNA in vivo, the level of pulmonary inflammation was evaluated, and the polarization of pulmonary macrophages was analyzed.

Results: The results showed that miR-184-3p was significantly downregulated in HP-exos, and supplementation of miR-184-3p enhanced the polarization of M1 macrophages, thus intensifying lung inflammation. HO-1 regulates the polarization of macrophages by regulating endothelial exosomes. Overexpression of HO-1 downregulates miR-184-3p, which negatively regulates Semaphorin 7A (Sema7a), which attenuated M1 type macrophages (M1) polarization and augmented M2 type macrophages (M2) polarization, thereby partially mitigating lung injury and inflammation.

Conclusion: Collectively, we elucidated a novel potential therapeutic mechanism that HO-1 alleviate inflammation by modulating the M1/M2 ratio in sepsis-induced ALI by regulating miR-184-3p/Sema7a expression.

Keywords: sepsis, acute lung injury, macrophage polarization, exosome, MiRNA

Introduction

Sepsis-associated acute lung injury (ALI) represents a prevalent and severe clinical syndrome characterized by a complex and incompletely understood pathogenesis, with mortality rates reaching up to 40%.[1] The polarization of alveolar macrophages between M1 (classical) and M2 (alternative) plays a crucial role in the pathogenesis of ALI.[2] Imbalanced polarization can trigger excessive inflammation, which strongly influences the development of sepsis-

Received: 5 December 2024
Accepted: 18 March 2025
Published: 18 April 2025

Graphical Abstract

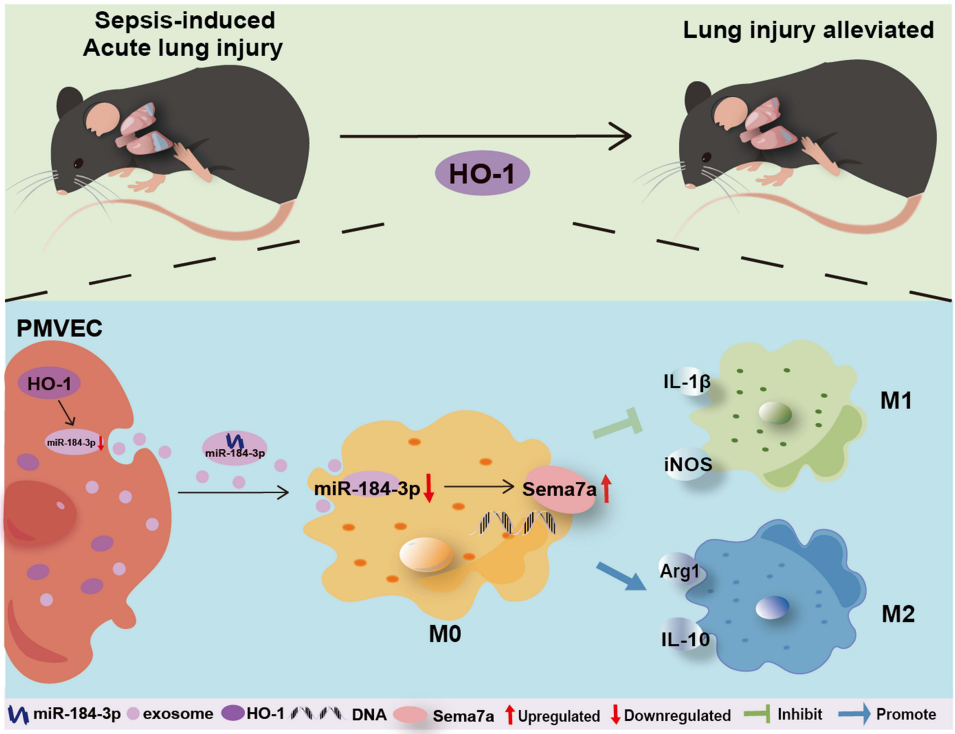

related organ damage and substantially affects clinical outcomes.[3] Cytokines released by these macrophages significantly impact the initiation and progression of sepsis-induced ALI.[4]

Pulmonary microvascular endothelial cells (PMVECs) constitute a uniform, continuous layer of thin endothelial cells, acting as a semi-permeable membrane, facilitating nutrient transport, regulating vascular permeability, and preserving microenvironmental equilibrium.[5] Recent studies have highlighted the additional immunoregulatory functions of PMVECs, including recruiting immune cells and participating in antigen presentation.[6–8] Particularly vulnerable to inflammatory damage during immune responses, the lungs, along with vascular endothelial cells in critical organs, are primary targets for inflammatory mediators.[9] In the physiological and pathological contexts of the lung, there is a sophisticated crosstalk between PMVECs and macrophages. Endothelial cells secrete bioactive substances that influence macrophage function and activity, while macrophages reciprocally modulate endothelial cell activities through phagocytosis, antigen presentation, and immune regulation.[10,11] This bidirectional interaction is crucial for maintaining normal lung function, defending against pathogen invasion, and lung diseases progression.[12] Our study is dedicated to elucidating the molecular mechanisms driving the interactions from the standpoint of macrophage polarization, as well as understanding how these dynamics are altered in acute lung injury, potentially offering novel preventative and therapeutic approaches for lung damage.

Exosomes are diminutive vesicles released by all cell types and are ubiquitously present in various bodily fluids.[13] They traverse to distant organs via blood and fluids, carrying diverse bioactive molecules from their cells to facilitate complex intercellular communication and play crucial roles in maintaining tissue function, regulating homeostasis, and modulating immune activities.[14–16] A distinctive feature of exosomes, setting them apart from other biological vesicles, is their rich content of nucleic acids, including miRNAs.[17] MiRNAs represent a novel class of short, endogenous non-coding RNAs that function as post-transcriptional regulators of gene expression, influencing numerous cellular signaling pathways,[18,19] serving as significant mediators of intercellular communication and influencing the pathogenesis of

various diseases.[20] However, the specific regulatory mechanisms and functions of exosomal miRNAs are still poorly understood, with limited studies focusing on their role in regulating the polarization of alveolar macrophages.

Heme oxygenase-1 (HO-1), an enzyme activated in response to stress, exerts an indispensable role in signaling and cytoprotective functions across a range of organs and tissues.[21,22] It has been documented to possess anti-inflammatory and antioxidant properties, facilitating the restoration of homeostasis following the onset of numerous pathological conditions.[23,24] Our prior research demonstrated that HO-1-derived carbon monoxide protects against sepsis-induced ALI,[25–27] and HO-1 can inhibit TXNIP/NLRP3 to affect macrophage polarization.[28] To further explore the interaction between endothelial cells and macrophages, considering the important role of exosomes in cell crosstalk, our research focuses on exosomes enriched with miRNAs to investigate how HO-1 protects and regulates the state and function of alveolar macrophages. These findings provide novel insights into the potential therapeutic applications of HO-1 and their intrinsic protective mechanisms in cases of lung injury.

Materials and Methods

Animals

In accordance with laboratory animal regulations, the Animal Care and Use Committee of Tianjin Nankai Hospital approved this study (Approval No. NKYY-DWLL-2022-031). Six-to-eight-week-old male C57BL/6J wild-type mice weighing 20–22 g were purchased from SPF (Beijing) Biotechnology Co., Ltd. HO-1 conditional knockout (HO-$1^{-/-}$) mice on a C57BL/6J background (HO-$1^{fl/fl/CAG}$-Cre^{ERT2}) were provided by Beijing Biocytogen Co., Ltd. HO-1 expression was induced by intraperitoneal injections of tamoxifen (10 mg/mL, Sigma-Aldrich) once daily for five consecutive days, followed by a one-week waiting period. All mice were maintained under controlled conditions at a temperature of 23 ± 2 °C, a 12-hour light/dark cycle, and with ad libitum access to water and food.

Lung Histological Analysis

The lung tissue was processed following standard histological procedures, including fixation, dehydration, embedding, and sectioning into 4 μm slices, followed by hematoxylin and eosin (H&E) staining. The sections were analyzed using a microscope (Leica, Germany). Assessment of ALI involved evaluating inflammatory cell infiltration, interstitial expansion, edema, and hemorrhage. Lung injury severity was graded on a scale from 0 to 4 as follows: none (0), mild (1+), moderate (2+), severe (3+), and extremely severe (4+), using a semiquantitative scoring system. Two pathologists who were blinded to the experimental protocol, independently assigned scores for each variable.

Lung W/D Ratio

The wet-to-dry weight ratio (W/D) was used to quantify the severity of pulmonary edema.[29] Initially, the wet weight (W) was measured, followed by determining the dry weight (D) after drying the tissue for 48 h at 65 °C.

Cell Culture and Treatments

MH-S cells, a mouse alveolar macrophage line (Procell, CL-0597, Wuhan, China), were cultured in Dulbecco's Modified Eagle Medium supplemented with 10% FBS and 1% penicillin–streptomycin (Gibco, 15,140–122) at 37 °C in a 5% CO_2 humidified environment. The cells were seeded in 96-or 6-well plates for subsequent experiments and allowed to grow until they reached 80–90% confluence. PMVECs (Procell, CP-M001, Wuhan, China) underwent identical cell handling procedures.

Exosome Isolation and Characterization

Exosomes were isolated from the supernatants of PMVECs cultured for 24–48h serum-free DMEM. The isolation procedure involved initial centrifugation of the PMVEC supernatants at 2,000×g for 30 min, followed by centrifugation at 10,000×g for 45 min to remove dead cells and cellular debris. Subsequently, the cell-free supernatant was further centrifuged at 100,000×g using a Beckman Coulter Optima ultracentrifuge (USA) for 1.5 h at 4 °C. The resulting exosome pellets were resuspended in PBS and stored at −80 °C.[30,31]

Exosomes suspended in PBS were applied onto 300-mesh copper grids and stained with 2% uranyl acetate. Images were acquired using a JEM-1010 electron microscope (JEOL, Tokyo, Japan) operating at an acceleration voltage of 100 kV. For each sample, 30 μL of diluted exosomes were mixed with 20 μL of fluorescently labeled antibodies (CD31, CD63, and CD81). The solution was mixed well and incubated in the dark at 37 °C for 30 min. Then, 1 mL of precooled PBS was added and the sample was centrifuged at 4 °C and 110,000×g for 70 min twice. The supernatant was discarded, and the pellet was resuspended in PBS. Once the sample was ready for detection, the protein indicator results and the size and particle concentration were obtained using the Flow NanoAnalyzer (NanoFCM, China).

Exosome Sorting Using CD31 Magnetic Beads

The remaining exosomes mentioned above were combined with CD31 microbeads at a volume ratio of 8:1, thoroughly mixed, and incubated at 4 °C for 30 min. Subsequently, 1 mL of PBS was added for resuspension. The resuspended exosome solution was loaded onto an LS column (Miltenyi Biotec, Germany) and washed with PBS. To collect the CD31-labeled exosomes, the solution was immediately pushed into the centrifuge tube using a plunger. The mixture was centrifuged at 100,000×g for 30 min at 4 °C. The supernatant was discarded, and the beads were resuspended in PBS. To separate the beads from the exosomes, elution buffer (0.1 M glycine, pH 2.8) was added, and after centrifugation at 10,000×g for 5 min, the supernatant containing the eluted exosomes was collected.

Labeling of Exosomes

Exosomes were labeled with DIR dye (Umibio, China), which emits a red color, following the manufacturer's instructions. Briefly, 1 μL of DIR dye was added to each milliliter of exosomes and incubated at 37 °C for 30 min. The labeled exosomes were then centrifuged at 100,000×g for 20 min. Following centrifugation, the pellet containing the labeled exosomes was diluted in PBS for subsequent experiments.[32]

Cellular Uptake of Exosomes

Labeled PMVEC-derived exosomes (100 μg/mL) were co-cultured with MH-S cells. After incubation for 24 h, the cells were fixed with 4% paraformaldehyde (PFA) for 30 min at 37 °C, washed thrice with PBS, and dyed the nucleus using DAPI. Finally, cell imaging was performed using a confocal microscope (Olympus FV1000, Japan), and SlideViewer software was utilized for image analysis.

In Vivo Atomized Inhalation of Exosomes

To investigate how macrophages phagocytize exosomes in lung tissue of mice, we used an aerosol inhalation device to administer labeled exosomes (6×10^{10} particles per mouse) for inhalation. The control group received an equal volume of PBS. Next, the fluorescence intensity of exosomes in the lungs was measured using an imaging technology (IVIS SPECTRUM, USA).

HO-1 Conditional Knockout Mice and Cecal Ligation and Puncture (CLP)

HO-1 conditional knockout ($HO\text{-}1^{-/-}$) mice on a C57BL/6J background were purchased from Beijing Biocytogen Co., Ltd. The CLP model was established following standard procedures.[33] Mice were anesthetized using isoflurane and underwent sterilization. An abdominal incision of 1 cm was made along the midline. The cecum was carefully extracted, ligated below the cecal valve, and punctured with an 18-gauge needle to induce sepsis. A small amount of cecal content was expelled before returning the cecum to the peritoneal cavity, followed by closure of the abdominal incision using sutures. All animals received subcutaneous fluid resuscitation with a saline solution (50 mL/kg) containing 0.2 mg/kg buprenorphine (Buprenex). Sham-operated animals underwent identical surgical procedures but without cecal ligation or puncture. After 24 h, animals were humanely euthanized with isoflurane, and lung tissues were collected for further analysis.

Cell Viability Assay

The viability of cells was assessed (5000 cells per tube) after injury and treatment using a Cell Counting Kit (CCK) from TransGen Biotech, following the manufacturer's instructions. MH-S cells were seeded at a density of 1×10^4 cells/mL in a 96-well plate and cultured at 37 °C with 5% CO_2. The cells were treated with different concentrations of Lipopolysaccharide (0, 0.1, 0.5, 1, 5, or 10 μg/mL) for 12 h. Subsequently, 10% of the total volume of CCK solution was added to each well and incubated for 4 h. After incubation, the absorbance was measured at 450 nm using a microplate reader.

MiR-184-3p Mimic/Agomir Transfection

To investigate the interaction between miR-184-3p and its target gene, MH-S cells were transfected with miR-184-3p mimics obtained from GenePharma (Shanghai, China; Table 1). The dry powder of the miR-184-3p mimic was dissolved in DEPC water following the manufacturer's instructions.[34] Next, 5 μL of miR-184-3p mimics and an equal amount of Lipofectamine® RNAiMAX (Invitrogen, USA) were separately diluted in 150 μL of DMEM. The diluted miR-184-3p mimics were then mixed with diluted Lipofectamine® RNAiMAX, incubated for 10 min, and added to six-well plates containing DMEM medium supplemented with 10% FBS, incubating for 48 h.

Animals in the miR-184-3p or NC groups were administered with 15 nmol (~10 mg/kg of 20 g) mmu-miR-184-3p agomir (GenePharma, China), or 15 nmol NC agomir, respectively.[35,36] Subsequently, bronchoalveolar lavage fluid (BALF) and lung tissues were collected for further analysis.

Lentiviral and miRNA Transfection

To induce HO-1 overexpression in PMVECs, cells were initially seeded at a density of 5×10^5 cells/flask and cultured in DMEM supplemented with 10% FBS and 1% antibiotics. Once the cells reached 40–50% confluence, they were ready for viral infection. The Hmox1-Mus-OE virus (GenePharma, China) was diluted 1:50 with culture medium. Polybrene was added to achieve a final concentration of 5 μg/mL. The original medium was aspirated from the flask, and the virus dilution was added to the cells, then incubated at 37 °C for 24 h. After incubation, the virus-containing medium was removed, and fresh medium was added to the cells, in a 37 °C incubator for further incubation.

Plasmids carrying Semaphorin 7A (Sema7a) and an empty control vector (GenePharma, China) were transfected into cells using jetPRIME® transfection reagent (Polyplus-transfection S.A., Illkirch, France), following the manufacturer's instructions. To prepare the transfection mixture, 2 μg of DNA plasmid was combined with 5 μL of miR-184-3p mimics in 200 μL of jetPRIME® buffer. Then, 4 μL of jetPRIME® reagent was added to the solution, which was vortexed briefly and centrifuged. The mixture was incubated at room temperature for 20 min. After incubation, the transfection mixture was added dropwise to the 6-well plates containing serum-rich medium. The cells were then incubated in a standard incubator for 24 to 48 h for further experimental procedures.

Flow Cytometry Analysis

Single-cell suspensions of lung tissue, Bronchoalveolar Lavage Fluid (BALF), and MH-S cells were prepared according to previously established methods.[26,28] Each cell suspension labeled with specific monoclonal antibodies: PE-F4/80 (catalog number 565410, BD, USA), FITC-CD11b (catalog number 557396, BD, USA), APC-Cy7-CD45 (catalog number 557659, BD, USA), PerCP-CD80 (catalog number 104722, Biolegend, USA), and APC-CD163 (catalog number

Table 1 Sequences of miR-184-3p Mimic/Agomir and NC Mimic/Agomir for Transfection

Gene	Sequence, 5'-3'	
	S	AS
miR-184-3p mimic/ agomir	UGGACGGAGAACUGAUAAGGGU	CCUUAUCAGUUCUCCGUCCAUU
NC mimic/ agomir	UUCUCCGAACGUGUCACGUTT	ACGUGACACGUUCGGAGAATT

https://doi.org/10.2147/IJN.S506830

155306, Biolegend, USA). Cell staining was performed in the dark for 20 min, followed by washing with PBS. The data were obtained using a BD FACSVerse flow cytometer (BD, USA) and analyzed using FlowJo v10 software (BD, USA).

Quantitative Real-time PCR (RT-qPCR)

Around 24–48 h after transfection, total RNA was isolated from cultured cells and lung tissue using the TransZol Up Plus RNA Kit (TransGEN, Beijing, China), following the manufacturer's instructions. Subsequently, the concentration and quality of RNA were assessed using a Nanodrop spectrophotometer (Thermo Scientific, Waltham, MA, USA).

For miRNA analysis, reverse transcription and RT-qPCR were performed using the Hairpin-it^{TM} miRNAs RT-qPCR Quantitation Kit (GenePharma, Shanghai, China) with specific primers. Similarly, for mRNA analysis, reverse transcription and RT-qPCR were performed using TransScript® One-Step gDNA Removal and cDNA Synthesis SuperMix (AT311, TransGEN, Beijing, China) and PerfectStart® Green qPCR SuperMix (AQ601, TransGEN, Beijing, China), respectively. The relative expression levels of miRNA/mRNA were determined using the $2^{-\Delta\Delta Ct}$ method, where U6/GAPDH served as internal controls for normalization (Table 2).

Western Blotting Analysis

Total protein was extracted using a total protein isolation kit (Solarbio, China), and its concentration was determined by the BCA method (Solarbio, China). First, 10 μg of protein per well was loaded onto a 10% SDS-PAGE gel for electrophoresis and subsequently transferred to polyvinylidene difluoride (PVDF) membranes (0.2 μM, Bio-Rad, USA). Next, the PVDF membrane was blocked for 15 min at room temperature and incubated with primary antibodies (Table 3) at 4 °C overnight. After washing, the membrane was treated with a secondary antibody (1:2000, sc-525409) for 1 h. Enhanced chemiluminescence (170–5070, Bio-Rad, USA) was used to visualize the bands, and band intensity was quantified using the Image J software.

Table 2 Primer Sequences of miRNA and mRNAs Oligomers for RT-qPCR

Gene	Primer Sequence,5'-3'	
	Forward	Reverse
iNOS	CATGCTACTGGAGGTGGGTG	CATTGATCTCCGTGACAGCC
Arg1	CTGAGCTTTGATGTCGACGG	TCCTCTGCTGTCTTCCCAAG
Sema7a	ACACACCGTGCTTTTCCATGA	CCTTTGTGGAGCCGATGTTC
Ralbp1	CGTCCTGTTCTGTCCCAATCA	GGCAGGAAGCACTCAGTCAT
Csf1r	CCTGCGATGTGTGAGCAATG	CGGATAATGAACCCTCGCCA
Atn1	AGTCTCCCTCGGATCTGGAC	CGGCACAGAAGGATGAGGTT
Csf1	TCCCATAAACCACATGCCCC	CCCAGCCATGTCGAAGAAGG
HO-1	CCTCACAGATGGCGTCACTT	TGGGGGCCAGTATTGCATTT
GAPDH	GGTTGTCTCCTGCGACTTCA	TGGTCCAGGGTTTCTTACTCC
miR-184-3p	UGGACGGAGAACUGAUAAGGGU	CCUUAUCAGUUCUCCGUCCAUU
miR-125b-5p	UUUUGCACCUGGAAUUCCAGCUU	AGGCUUUAGUCCCUGGUUUCAAUU
miR-203-5p	AGUGGUUCUUGACAGUUCAACA	UUGAACUGUCAAGAACCACUUU
U6	CAGCACATATACTAAAATTGGAACG	ACGAATTTGCGTGTCATCC

Table 3 List of the Primary Antibodies Used in This Study

Antibody	Catalogue number	Brand	MW (kDa)	Application
F4/80	29,414-1-AP	Proteintech	NA	IF
iNOS	ab178945	abcam	NA	IF
Arg1	16001-1-AP	Proteintech	NA	IF

(*Continued*)

Table 3 (Continued).

Antibody	Catalogue number	Brand	MW (kDa)	Application
β-actin	ET1702-67-100	HUABIO	42	WB
HO-1	10,701-1-AP-100	Proteintech	33	WB IF
Sema7a	Ab23578	abcam	75	WB IF

Immunofluorescence (IF)

After the mice were euthanized, intact lung tissue was fixed in 4% PFA overnight. The tissue was then dehydrated using a sucrose gradient, embedded, and sliced to the appropriate thickness using a −20 °C frozen slicer for subsequent immunofluorescence staining. Antigen retrieval was performed in a pressure cooker using EDTA antigen repair buffer (pH 9.0). Following natural cooling, the slides were washed three times in PBS (pH 7.4) by shaking and soaking. A histochemical pen was used to draw a circular boundary around the tissue, and 1% BSA was added within the boundary to ensure even coverage. The slides were sealed at room temperature for 1 h, primary antibodies (Table 3) were added to the tissue sections, which were then incubated overnight at 4 °C in a wet box. Subsequently, the sections were washed three times in PBS (pH 7.4) with shaking and soaking. Excess liquid was gently shaken off, and secondary antibodies were added within the outlined area, covering the tissue while avoiding light exposure. The slides were incubated at room temperature in the dark for 1 h. Finally, nuclei were counterstained with DAPI (1:1000, Beyotime, China), and the slides were prepared for observation and sealing.

Enzyme-Linked Immunosorbent Assay (ELISA)

MH-S cells were treated and cultured according to established protocols. After cultivation, the culture medium was collected and centrifuged at 300×g for 5 min at 4 °C. The resulting supernatants were carefully collected. The levels of IL-1β and IL-10[37,38] released were quantified using ELISA kits (RX203063M, RX203075M, Ruixinbio, China), following the manufacturer's instructions. Similarly, the supernatant from mouse BALF was analyzed using ELISA kits (MLB00C, DY417-05, R&D Systems, USA).

Sequencing of Exosomal miRNAs

Total RNA was extracted and purified from the lungs of three groups (Ctrl, CLP, and HO-1$^{-/-}$+CLP) collected 48 h after CLP. The quality of the RNA was assessed before preparing small RNA sequencing libraries using the PE150 sequencing protocol. Library quality was further evaluated with FastQC, and subsequent sequence processing involved trimming, q20 filtering, and adaptor removal using fastp. To eliminate rRNA, tRNA, and other ncRNAs, sequences were aligned against the Rfam database using Bowtie. Quantitative analysis of small RNAs was performed using miRDeep2, and DESeq2 was used for differential expression analysis. Differentially expressed miRNAs were identified by performing t-tests, with significance defined as |log2Foldchange|>1 and $P<0.05$. Pathway analysis was conducted using the Gene Ontology (GO) database for functional annotation.

Prediction and Identification of miRNA–mRNA Targeting Relationships

Databases Starbase 3.0 and DisGeNET were jointly used to predict the target genes of miR-184-3p. To validate these predictions, dual-luciferase reporter assays were used. The 3'-UTR sequences of Sema7a, containing both the predicted miR-184-3p binding sites and their corresponding mutants, were cloned into a plasmid vector and transfected into HEK293 cells. Along with these constructs, a Renilla luciferase vector was co-transfected to normalize transfection efficiency. Luciferase activity was measured in relative light units, where the activity of Photinus pyralis firefly luciferase was normalized to that of the Renilla luciferase vector.[34]

Statistical Analysis

In this study, all outcomes are presented as the mean ± SD of at least three independent experiments, with the sample size of each experiment detailed in the accompanying figure legends. The statistical analyses were conducted utilizing GraphPad Prism 8 software, including normality assessments for all datasets. For normally distributed data, one-way ANOVA was employed to compare multiple groups, and unpaired Student's *t*-test (two-tailed) for comparing two groups. If the data did not follow a normal distribution, the Mann–Whitney rank-sum test was applied. Survival rates were depicted using Kaplan-Meier curves, and comparisons of survival curves were performed with a log-rank (Mantel-Cox) test. Statistical significance was considered at a P value <0.05.

Results

Exosome Extraction, Identification and Phagocytosis by Macrophages

Exosomes were successfully isolated from mouse lung tissue using the described method (Figure 1A and B), and CD31 magnetic beads were used to isolate endothelial exosomes (Figure 1C). The morphological integrity and particle size of exosomes were confirmed by transmission electron microscopy (TEM) and nanoparticle tracking analysis (NTA) before and after sorting (Figure 1D, Table S1). The results showed that although the particle size of exosomes decreased after sorting, their morphology remained intact. These data indicate that the exosomes have been successfully extracted and identified.

DIR-labeled exosomes (100 μg/mL) were co-cultured with MH-S macrophages for 24 h, and then observed under a confocal microscope (Figure 1E and F). Additionally, a custom-built nebulizer was designed for aerosolizing exosomes (Figure 1G, Figure S1). After depilation, lung fluorescence intensity was assessed in prone mice. Per mouse, 6×10^{10} exosome particles were selected for inhalation.[39–41] Following euthanasia, vital organs such as the heart, liver, lungs, and kidneys were harvested to measure fluorescence intensities (Figure 1H). The analysis indicated that lung fluorescence intensities were significantly higher in the exosome inhalation group, indicating effective lung delivery. Furthermore, Immunofluorescence staining of lung tissue sections showed an increase in DIR fluorescence intensity in the CLP +PMVEC-exo group, suggesting efficient alveolar macrophage phagocytosis of exosomes (Figure 1I). The aforementioned results demonstrate that macrophages can capture exosomes both in vivo and in vitro.

MiR-184-3p Promotes the M1 Phenotype and Inhibits the M2 Phenotype in Macrophages

To investigate the miRNAs involved in sepsis-induced lung injury, microarray assays were performed on PMVEC-exo (Figure S2A). A heat map analysis and clustering (Figure S2B-C) highlighted differences between the control and CLP groups, identifying differentially expressed genes (DEGs) (Figure 2A) and the top 10 genes as shown in Table S2. Validation focused on the top three differentially expressed miRNAs, confirming that miR-184-3p had the most significant down-regulation in CLP group (Figure S2D-G). Gene Ontology (GO) analysis revealed enrichment in 16 biological processes, including inflammation-related pathways (Figure 2B). Lipopolysaccharide (LPS)-treated endothelial exosomes were analyzed by TEM, NTA (Figure S2H-I). The exosome isolation and characterization procedures were performed in accordance with MISEV2023 guidelines,[30] and then NanoFCM was used to validate exosome markers (CD63 and CD81) due to its high sensitivity and minimal sample requirements (Figure 2C), with RT-qPCR assays indicating significant downregulation of miR-184-3p (Figure 2D).

To induce macrophage polarization towards M1 (classically activated) or M2 (alternatively activated/anti-inflammatory) phenotypes, various stimulatory agents such as IL-4 (20 ng/mL)[42,43] for M2 and LPS for M1 were utilized. MH-S cells were pretreated with LPS at different concentrations (0, 0.1, 0.5, 1.0, 5, or 10 μg/mL) for 12 h, revealing reduced survival at 5 and 10μg/mL and a concentration-dependent increase in iNOS (Inducible Nitric Oxide Synthase) expression at 5μg/mL (Figure S3A-B), which was chosen for further studies.

To evaluate the role of exosomes from LPS-stimulated PMVEC in macrophage polarization, treating endothelial cells were treated with LPS (10 μg/mL)[44,45] for 24h. Exosomes were isolated and co-cultured with MH-S cells, which showed decreased miRNA-184-3p levels (Figure 2E). Flow cytometry demonstrated an increase in the anti-inflammatory M2 phenotype (CD163+) in the LPS-treated group (Figure 2F), with RT-qPCR confirming elevated Arg1 (Arginase 1) and

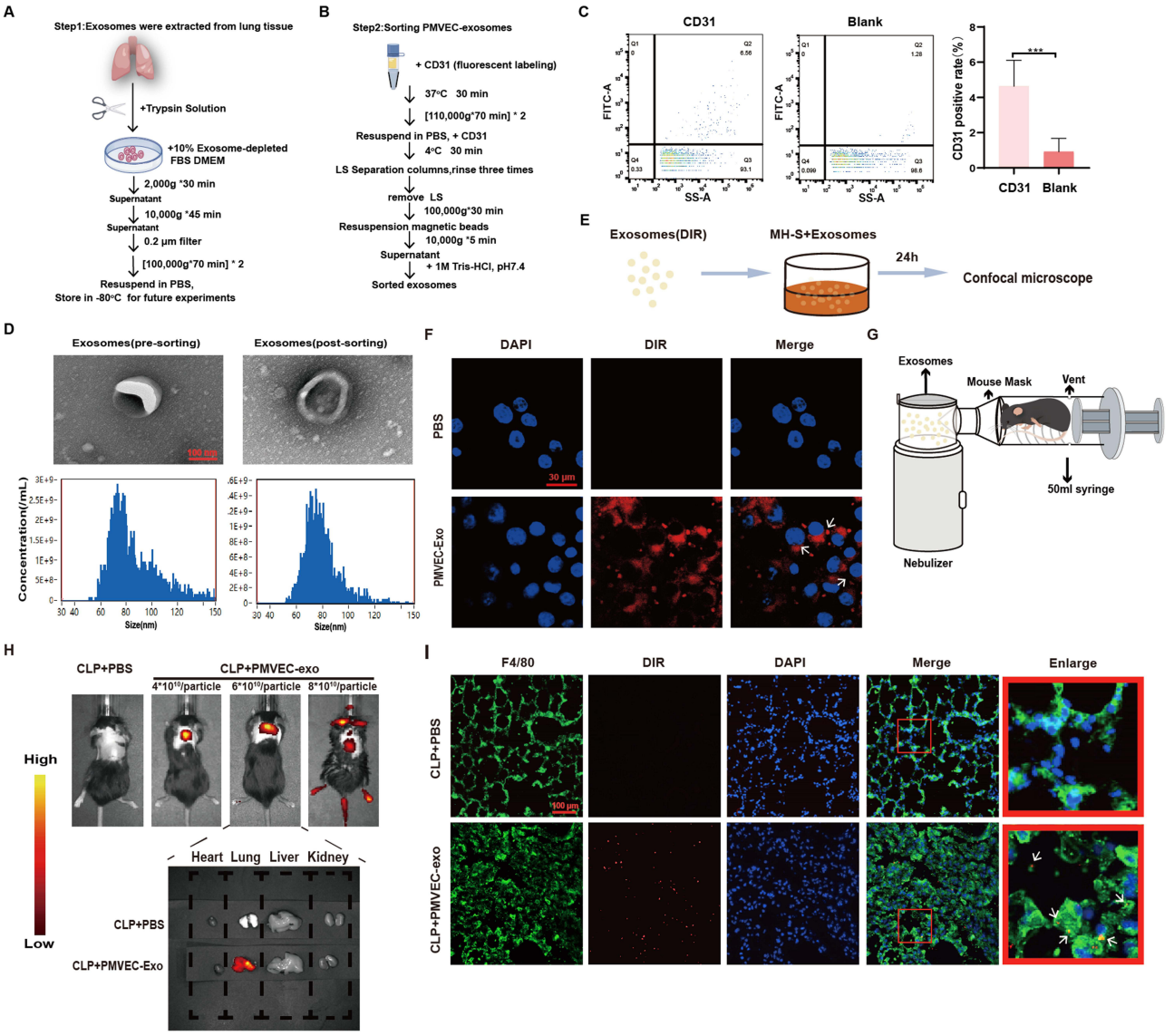

Figure 1 Exosome extraction, identification and phagocytosis by macrophages (**A**) Extraction of exosomes from lung tissue. (**B**) Schematic of the sorting process for PMVEC-derived exosomes. (**C**) Flow cytometric analysis for the isolation of CD31+ exosomes (n=6). (**D**) Characterization of exosomes isolated from lung tissue/PMVEC via TEM (scale bar=100 nm) and NTA. (**E**) Experimental schematic for macrophage capture of PMVEC-derived exosomes. (**F**) Observation of exosome phagocytosis by macrophages using confocal microscopy (scale bar=30 μm, n=3). (**G**) Schematic of the custom-built mouse nebulizer. (**H**) Utilization of small animal imaging technology demonstrated increased fluorescent intensity. (**I**) Immunofluorescence staining displaying F4/80 (green), DIR (red), and DAPI (blue) with a scale bar of 100 μm. Data are presented as mean±SD and statistically analyzed using Student's *t*-test. ***P<0.001.

reduced iNOS expression. ELISA was performed to quantify the levels of the cytokines IL-1β and IL-10, which are required for driving macrophage polarization.[46] The results revealed decreased IL-1β and increased IL-10 in the LPS-stimulated group (Figure 2G). These findings indicate that exosomes from LPS-stimulated-PMVECs modulate macrophage polarization and may alleviate cellular inflammation.

To elucidate the effect of miR-184-3p, MH-S cells were transfected with the miR-184-3p mimic (Figure 2H), resulting in an increase in CD80+ macrophages and a decrease in CD163+ macrophages (Figure 2I), along with elevated iNOS and IL-1β expression, reduced Arg1 and IL-10 levels (Figure 2J). These findings suggest that miR-184-3p promotes M1 polarization and suppresses the M2 phenotype, potentially intensifying inflammatory responses.

https://doi.org/10.2147/IJN.S506830

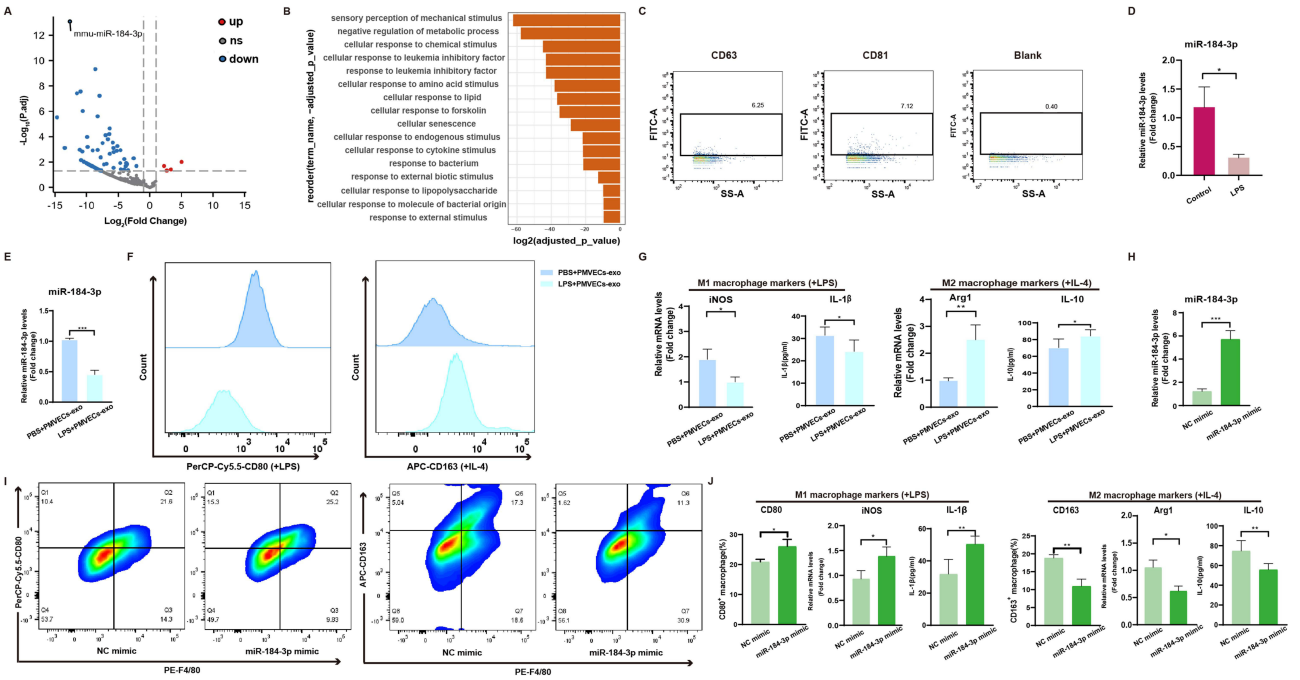

Figure 2 Effects of miR-184-3p overexpression on macrophage M1/M2 polarization (**A**) Volcano plot illustrating differentially expressed genes (n=3). (**B**) GO analysis of pathways enriched by miR-184-3p target genes. (**C**) Nano-flow cytometric detection of exosomal markers CD63 and CD81. (**D**) Quantitative analysis of miR-184-3p expression levels (n=6). (**E**) Macrophages were co-cultured with PMVEC-derived exosomes treated with LPS or PBS for 24 h to assess changes in miR-184-3p expression levels (n=6). (**F**) Co-culture with PMVEC-derived exosomes treated with LPS or PBS, the counts of M1 (CD80+) and M2 (CD163+) macrophages was quantified using flow cytometry. (**G**) RT-qPCR was utilized to measure the expression of iNOS and Arg1 (n=6). ELISA assays quantified the levels of IL-1β and IL-10 in the culture supernatant (n=5). (**H**) Comparative expression levels of miR-184-3p in NC mimic and miR-184-3p mimic groups (n=6). (**I-J**) Proportions of F4/80+ CD80+ and F4/80+ CD163+ macrophages assessed via flow cytometry (n=3), RT-qPCR was employed to evaluate the expression of iNOS and Arg-1 (n=6), ELISA quantification of IL-1β and IL-10 levels in the supernatant (n=5). Data are presented as mean ± SD and analyzed using Student's *t*-test. *P<0.05, **P<0.01, ***P<0.001.

MiR-184-3p Downregulates Sema7a to Promote M1 and Inhibit M2 Polarization in Macrophages

Using Starbase 3.0 and DisGeNET, target genes (Ralbp1, Csf1R, Atn1, Sema7a, and Csf1) for miR-184-3p were obtained (Figure 3A and B) and then experimentally validated. In MH-S cells, transfection with a miR-184-3p mimic significantly reduced Sema7a mRNA levels (Figure 3C). Gene prediction tools identified binding sites for miR-184-3p on Sema7a (Figure 3D). Dual-luciferase reporter assays further confirmed that miR-184-3p significantly suppressed the luciferase activity of the Sema7a 3'-UTR WT construct (Figure 3E). Western blotting analysis of MH-S cells corroborated these findings (Figure 3F and G). In Figure 3H, green and red fluorescence signals represent macrophages (F4/80) and Sema7a, respectively. The colocalization of these signals indicates their spatial proximity and interaction. The fluorescence intensity trend analysis demonstrates that miR-184-3p reduces Sema7a expression, as shown by the lower red fluorescence intensity compared to the green signal. Additionally, after pooling BALF, alveolar macrophages were isolated via flow cytometry (Figure S4). The levels of Sema7a mRNA from BALF alveolar macrophages were lower in the miR-184-3p agomir group (Figure 3I).

The study investigated the influence of Sema7a, a target gene of miR-184-3p, on macrophage polarization and inflammatory responses. Initially, macrophages with Sema7a overexpression were constructed (Figure 3J and K). Transfection with the miR-184-3p mimic increased the counts of M1 polarization (CD80+), but this effect was countered by simultaneous transfection with a Sema7a overexpression vector (Figure 3L). Moreover, co-transfection reduced the expression levels of iNOS and IL-1β while increasing the levels of Arg1 and IL-10 (Figure 3M), demonstrating that miR-184-3p negatively regulates Sema7a. As a result, it can be concluded that miR-184-3p downregulates Sema7a, promotes M1 polarization of macrophages and inhibits M2 polarization.

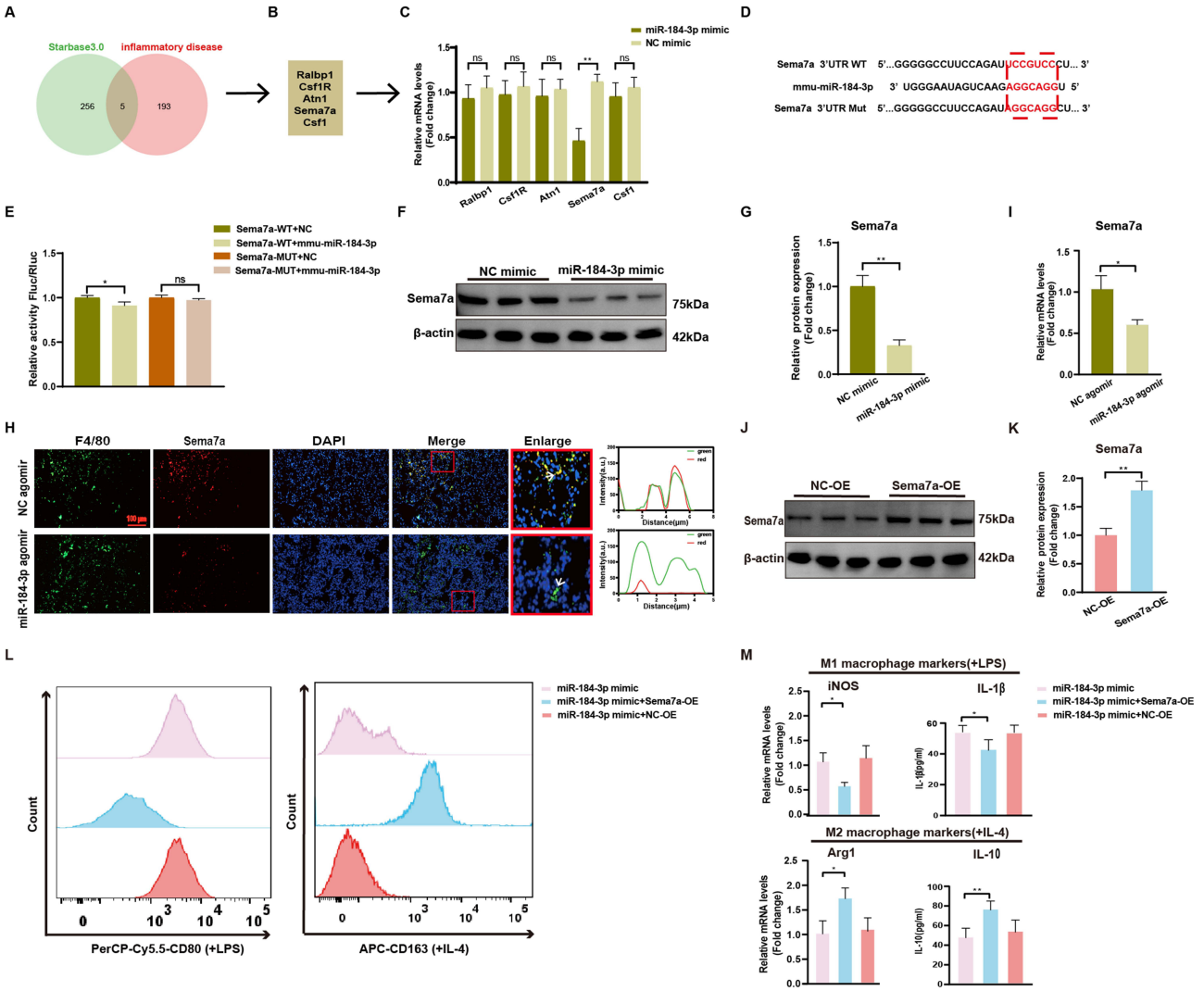

Figure 3 MiR-184-3p negatively regulates Sema7a to promote M1 and inhibit M2 polarization of macrophages. (**A-B**) Predictive analysis using starBase 3.0 identified 261 candidate genes potentially targeted by miR-184-3p. Intersection with 198 inflammation-related from DisGeNET yielded five candidate genes. (**C**) RT-qPCR analysis of these five candidate genes was performed in MH-S cells transfected with either miR-184-3p mimic or NC mimic (n=6). (**D-E**) Co-transfection of miR-184-3p and PmirGLO-sema7a-WT/MUT reporter plasmids into 293T cells revealed significant differences in the expression levels of the sema7a-WT wild-type luciferase reporter gene compared to the NC group (n=3). (**F-G**) Western blot analysis and protein quantification were employed to assess Sema7a levels. (**H**) Immunofluorescence staining was used to visualize F4/80 (green), Sema7a (red), and DAPI (blue) across various groups (scale bar=100 μm, n=3). (**I**) RT-qPCR was conducted to measure Sema7a expression (n=6). (**J-K**) Western blot analysis were conducted to assess Sema7a levels. (**L**) Counts of CD80+ and CD163+ macrophages were determined via flow cytometry. (**M**) mRNA levels of iNOS and Arg-1 (n=6), ELISA quantified the secretion levels of IL-1β and IL-10 in the supernatants (n=6). Data are presented as mean±SD and analyzed using Student's *t*-test and one-way ANOVA. *P<0.05, **P<0.01.

Overexpression of HO-1 Regulates Macrophage Polarization by Downregulating miR-184-3p

In previous studies, we observed increase an HO-1 expression in the lungs during LPS-induced ALI, indicating its role in endogenous pulmonary protection.[27,47,48] After confirming the successful construction of HO-1 knockout mice (Figure S5A), exosomes from lung endothelial cells of CLP and HO-1$^{-/-}$+CLP mice were sequenced for miRNA. A volcano plot analysis revealed a significant upregulation of miR-184-3p in HO-1$^{-/-}$+CLP group (Figure 4A) and the top 10 genes were shown in Table S2. To further investigate the role of HO-1 in the progression of ALI, HO-1 was overexpressed in endothelial cells, as determined by immunofluorescence (Figure 4B), mRNA (Figure 4C) and protein levels (Figure 4D and E).

To research the regulatory relationship between HO-1 and miR-184-3p, exosomes from HO-1/PMVEC or NC/PMVEC were analyzed. The expression levels of miR-184-3p did not differ between the NC-PMVEC and PMVEC

https://doi.org/10.2147/IJN.S506830

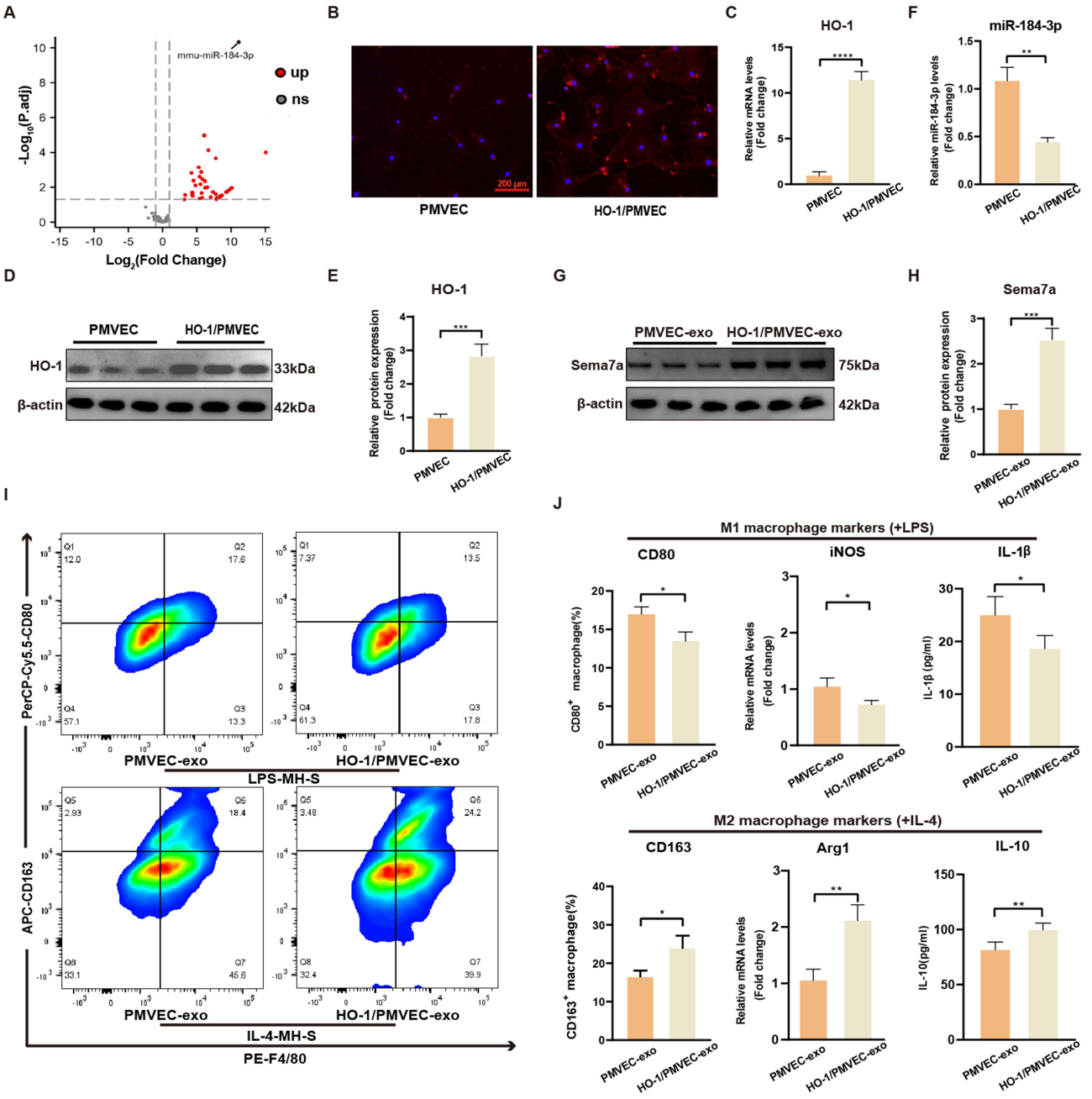

Figure 4 Regulation of Macrophage Polarization by HO-1-Modified PMVECs via Downregulation of miR-184-3p. (**A**) Volcano plot illustrating differentially expressed genes (n=3). (**B**) Immunofluorescence labeling for HO-1. (**C**) mRNA expression levels of HO-1 (n=6). (**D-E**) Western blot analysis and protein quantification for HO-1. (**F**) Expression levels of miR-184-3p (n=6). (**G-H**) Western blot analysis and protein quantification for Sema7a. (**I-J**) Proportions of F4/80+ CD80+ and F4/80+ CD163+ macrophages assessed via flow cytometry (n=3). Expression levels of iNOS and Arg-1 (n=6), ELISA quantification of IL-1β and IL-10 secretion levels in supernatants (n=5). Data are presented as mean±SD and analyzed using Student's *t*-test. *P<0.05, **P<0.01, ***P<0.001, ****P<0.0001.

groups (Figure S5B). As illustrated in Figure 4F, miR-184-3p expression was lower in exosomes from HO-1/PMVEC. Further analysis concentrated on the HO-1 and Sema7a interaction, co-culturing HO-1/PMVEC-exo (HP-exos) with MH-S cells enhanced Sema7a expression (Figure 4G and H).

The effect of HP-exos on macrophage polarization was evaluated by co-culturing with MH-S cells stimulated with LPS/IL-4. Flow cytometry analysis demonstrated a significant increase in the M2 phenotype (F4/80+ CD163+) and a decrease in the M1 phenotype (F4/80+ CD80+), as confirmed by an increase in Arg1 and IL-10 and a decrease in iNOS

and IL-1β (Figure 4I and J). These results suggest that HO-1 influence macrophage polarization and mitigate inflammatory responses by downregulating miR-184-3p.

Hemin Regulates Macrophage Polarization in Lung Tissue by Downregulating Endothelial Exosomal miR-184-3p

Considering the potential clinical application of HO-1, we further investigated the role of the HO-1 agonist Hemin in ALI. Using Cecal ligation perforation (CLP) model mice, there was no difference in miR-184-3p levels between the control group and the sham operation group (Figure S6A). Intraperitoneal injection of 30 mg/kg Hemin (Sigma, USA) 2 hours before CLP,[28,49,50] and Hemin pretreatment decreased miR-184-3p levels and enhanced Sema7a expression in lung tissue (Figure 5A and B). Histological analysis revealed CLP-induced lung injury with thickened alveolar septa, inflammation, edema, congestion, and hemorrhage, which were alleviated by Hemin pretreatment (Figure 5C and D). This was supported by reduced lung injury scores, and wet-to-dry weight ratios (Figure 5E and F). ELISA results of BALF showed higher IL-1β and lower IL-10 levels in the CLP group; however, Hemin pretreatment reversed this pattern (Figure 5G and H). Survival analysis post-modeling for 7 days

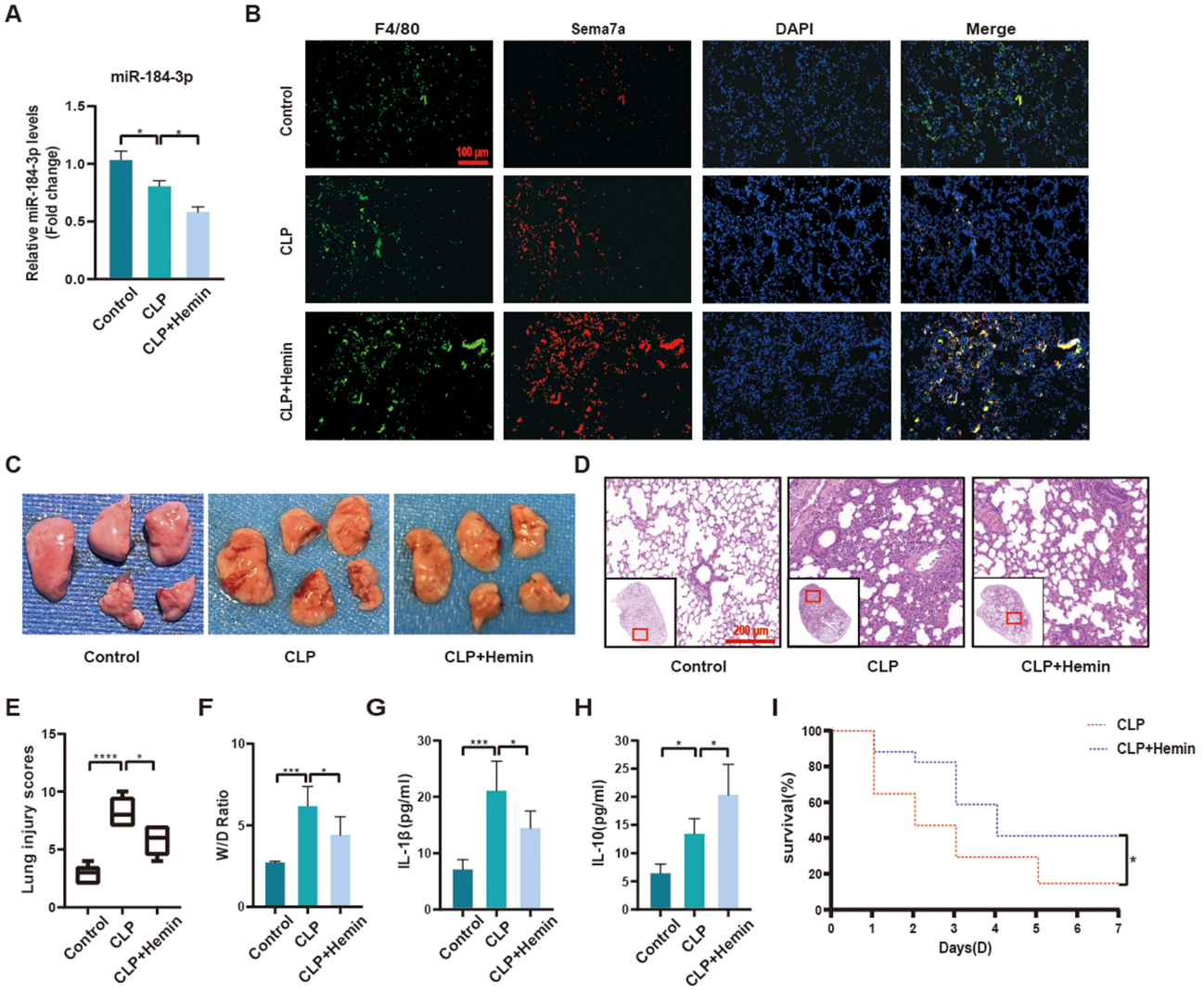

Figure 5 HO-1 agonist Hemin reduces lung tissue inflammation by regulating miR-184-3p. (**A**) Expression levels of miR-184-3p (n=6). (**B**) Immunofluorescence staining showing F4/80 (green), Sema7a (red), and DAPI (blue) across various groups, (scale bar=100 μm, n=3). (**C**) Representative photograph of mouse lung tissues illustrating injury severity (n=3). (**D**) Histopathological alterations in lung sections, highlighted by H&E staining (scale bar=200 μm, n=3). (**E**) Semi-quantitative assessment of lung tissue damage using lung injury scores via the Mann–Whitney *U*-test. (**F**) Measurement of lung wet/dry weight ratio (W/D) in rats. (**G-H**) ELISA quantification of IL-1β and IL-10 levels in BALF supernatant (n=5). (**I**) Survival enhancement in CLP mice treated with Hemin (n=15). Data expressed as mean±SD, analyzed using Student's *t*-test and one-way ANOVA. *P<0.05, ***P<0.001, ****P<0.0001.

https://doi.org/10.2147/IJN.S506830

indicated a higher survival rate in the Hemin pretreatment group (Figure 5I). Flow cytometry and immunofluorescence assessments showed Hemin favorably modulated macrophage polarization, reducing M1 and increasing M2 phenotypes (Figure S6B and Figure 6A – C), with corresponding changes in iNOS and Arg1 expression (Figure 6D and E). Collectively,

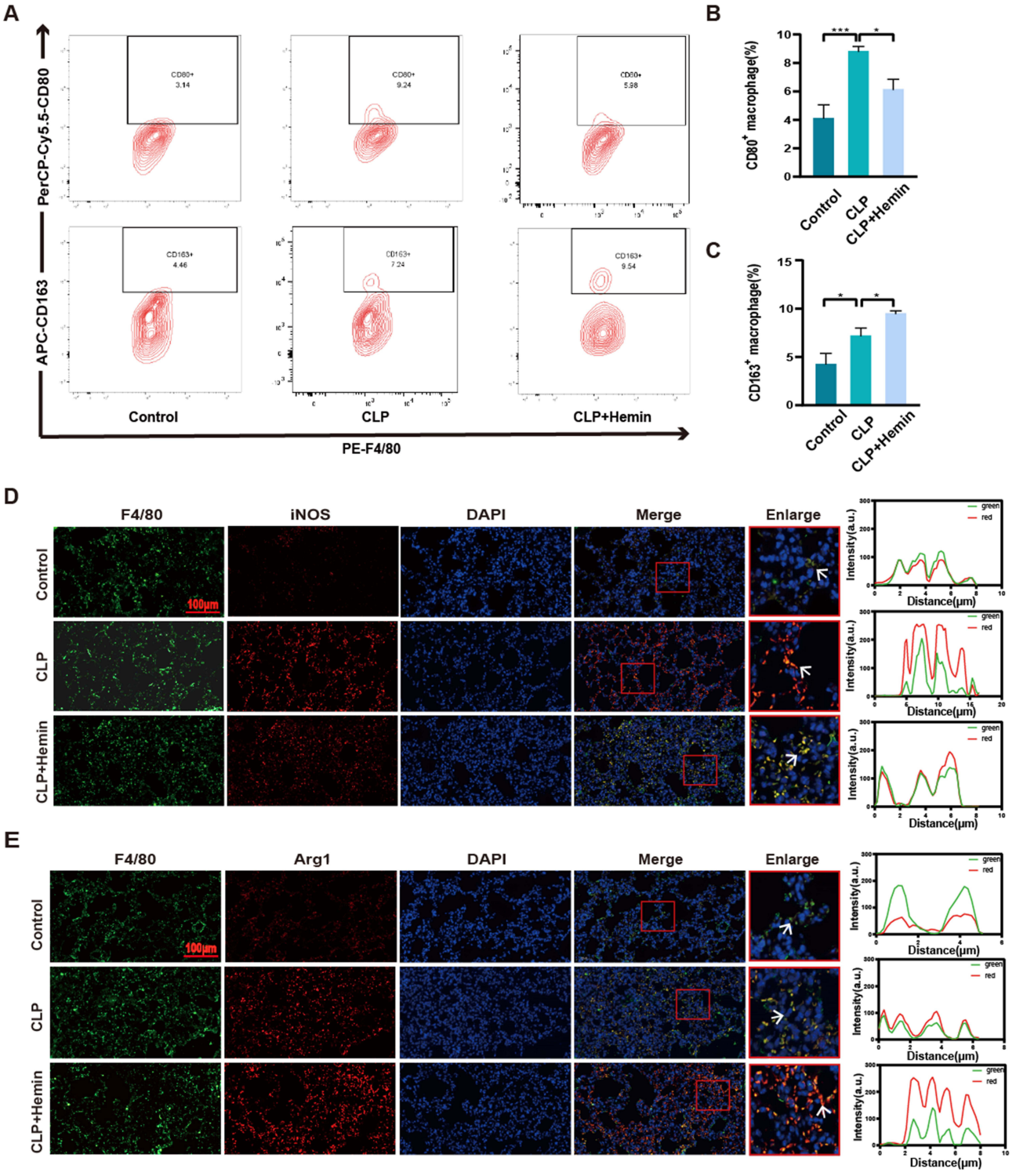

Figure 6 Regulatory effects of HO-1 agonist Hemin on macrophage polarization in lung tissues. (**A-C**) Flow cytometric analysis to determine the ratio of F4/80+CD80+ to F4/80+CD163+ macrophages (n=3). (**D-E**) Immunofluorescence staining for F4/80 (green), iNOS (red), Arg1 (red), and DAPI (blue) in different groups (scale bar=100 μm, n=3). Data expressed as mean±SD, analyzed using Student's *t*-test and one-way ANOVA. *P<0.05, ***P<0.001.

these findings underscore the potential of HO-1 activation by Hemin to modulate macrophage polarization and mitigate inflammatory responses in a murine model of ALI.

Discussion

Acute lung injury (ALI) is characterized by extensive airway inflammation, persistent hypoxemia, tissue disruption, and dyspnea.[51] The cecal ligation and perforation (CLP) model closely imitates sepsis mechanisms and is considered to be the gold standard.[33] In our study, mice exhibited increased ocular secretions, more frequent shivering, reduced scratching behavior, and sluggish movement 24 h after CLP. These observations indicated severe physiological disturbances caused by sepsis, and affected mice displayed pulmonary inflammation and injury, including collapsed alveolar structures, thickened alveolar septa, altered membrane transparency, and infiltration of a large number of inflammatory cells.

Nebulization provides significant advantages in terms of targeted delivery, localized drug concentration, safety, and patient tolerability, establishing it as the optimal route for exosome administration in sepsis-induced lung injury.[52–54] While our study primarily focuses on lung targeting, we recognize that systemic distribution of exosomes, could have implications for non-target organs, such as the liver. However, our findings demonstrate that nebulization effectively minimizes exosome distribution to these non-target organs, ensuring that therapeutic effects are predominantly concentrated in the lungs. This targeted approach not only enhances therapeutic efficacy but also reduces the risk of unintended interactions or systemic side effects in other organs, further underscoring the clinical relevance of nebulization for lung-specific therapies.

The pathogenesis and potential treatments for sepsis-induced ALI have been extensively investigated. The phenotypic transformation of alveolar macrophages plays a crucial role in ALI.[55] M1 macrophages exhibit proinflammatory and antipathogenic effects, while M2 macrophages contribute to tissue remodeling and profibrotic processes. Therefore, an imbalance favoring M1 macrophages exacerbates lung inflammation, whereas the dominance of M2 macrophages reduces lung injury. However, the optimal strategy for managing inflammation and improving patient outcomes remains unclear. Our previous studies highlighted HO-1 as an essential endogenous protective factor[48] and found that HO-1 and its byproduct, carbon monoxide (CO), significantly ameliorate organ damage induced by endotoxins in the lungs, heart, and kidneys, and notably enhance survival rates. These beneficial effects are thought to involve increased antioxidant enzyme activity, reduced lipid peroxidation, anti-apoptotic effects, and suppression of inflammatory responses. Furthermore, HO-1 alleviates endotoxin-induced ALI by modulating the M1/M2 polarization of alveolar macrophages during inflammation.[28]

Endothelial cell damage, particularly in PMVECs, is a critical factor in causing high-protein pulmonary edema and subsequent lung dysfunction in ALI.[56,57] Studies have shown that IL-1β-activated PMVECs regulate the polarization of skin macrophages during systemic sclerosis.[58] However, there is limited research on the interaction between signaling factors released by endothelial cells, such as exosomes, and macrophages. Macrophage polarization is strongly influenced by exosomal miRNAs,[59,60] which act as post-transcriptional regulators of gene expression and participate in the modulation of various cellular signaling pathways. Hence, our study aims to provide greater insights into the mechanisms involving HO-1 and elucidate the mechanism of HP-exo in alleviating lung injury.

Exosomes isolated from lung microvascular endothelial cells showed a reduction in miR-184-3p levels in the CLP group compared to the control group. Astonishingly, compared to HO-1 knockout mice, the expression of miR-184-3p increased in the CLP group, and this difference drew our attention. Our previous research found that endogenous HO-1 levels increase in CLP/LPS-induced inflammatory models.[28,48] To investigate the correlation between HO-1 and miR-184-3p, transcriptome sequencing was conducted on endothelial cell exosomes from HO-1 knockout mice, and HO-1-overexpressing endothelial cells were used to assess miR-184-3p expression changes during CLP/LPS-induced ALI. Our results indicated that HO-1 can suppress miR-184-3p expression in ALI. In addition to previous findings highlighting the role of miR-184-3p in communication between tumor cells and macrophages,[61,62] our study suggested that HO-1 might regulate alveolar macrophage polarization through exosome-derived miR-184-3p secreted by lung microvascular endothelial cells.

We found that introducing the miR-184-3p mimic not only suppressed Sema7a expression in MH-S cells but also downregulated Sema7a in CLP mice treated with the miR-184-3p agomir. Flow cytometry analysis, RT-qPCR, and

ELISA revealed that miR-184-3p significantly promoted M1 macrophage polarization while inhibiting M2 macrophage polarization. Semaphorins, a group of proteins comprising eight distinct subfamilies, were initially identified for their role in guiding axons during neurogenesis.[63] Among these, Sema7a, an immune semaphorin, plays a pivotal role in regulating various immunoinflammatory processes, including immune cell interactions, inflammatory infiltration, and cytokine production.[64] While previous studies suggested Sema7a acts as a negative regulator of macrophage activation and IL-10 expression,[65] our research revealed that Sema7a drives alveolar macrophages toward the non-classical M2 phenotype, characterized by decreased proinflammatory cytokine levels and increased IL-10 and Arg1 expression. The function of Sema7a varies depending on the target receptors expressed in different tissues, prompting our future research to explore its broader implications beyond macrophages alone.

This study has certain limitations. Further investigations are necessary to confirm the effects of HO-1 on other lung inflammatory cells, such as lymphocytes and neutrophils, which are closely linked to lung injury. Detailed studies are essential to elucidate the specific mechanism through which HO-1 regulates Sema7a by modulating miR-184-3p. Moreover, we studied the M2 group without subdivision and should be more rigorous and detailed in the future. At the same time, miRNAs are not the only substances in exosomes that are involved in this process, and other mechanisms might be involved in the regulation of macrophage polarization by exosomes.

To summarize, we demonstrated that overexpression of HO-1 increases Sema7a expression by downregulating miR-184-3p, thereby exerting an anti-inflammatory effect on lung tissue. This modulation reduces M1 polarization and enhances M2 polarization of alveolar macrophages, which helps alleviate the inflammatory response, mitigate lung injury, and improve outcomes in sepsis-induced ALI. Our findings provided a theoretical basis for the therapeutic potential of the HO-1 agonist Hemin in treating ALI during sepsis at the cellular interaction level. In the future, we aim to systematically and effectively investigate exosome aerosolization technology.

Conclusion

In summary, in vitro, we induced polarization of alveolar M1 macrophages with LPS and promoted M2 macrophage polarization with IL-4. Our findings showed that HO-1/PMVEC-derived exosomes (HP-exos) effectively inhibit M1 polarization and promote M2 polarization by downregulating miR-184-3p and upregulating Sema7a. This modulation partially alleviates sepsis-induced ALI and reduces inflammatory responses. Furthermore, our research elucidates the mechanism of HO-1 modified exosomes in the crosstalk between cells and provides innovative evidence for the potential therapeutic application of HP-exos in treating inflammation, highlighting their effectiveness as therapeutic targets for ALI.

Abbreviations

ALI, Acute lung injury; Arg1, Arginase 1; ARDS, Acute respiratory distress syndrome; BALF, Bronchoalveolar lavage fluid; CCK, Cell Counting Kit; CLP, Cecal ligation and puncture; DEG, Differentially expressed genes; ELISA, Enzyme-linked immunosorbent assay; Exo, Exosome; FCM, Flow cytometry analysis; GO, Gene ontology; HO-1, Heme oxygenase oxygen-1; HP-exo, HO-1/PMVECs-derived exosomes; IF, Immunofluorescence; IL, Interleukin; iNOS, Inducible Nitric Oxide Synthase gene; LPS, Lipopolysaccharide; M1, M1 type macrophages; M2, M2 type macrophages; miRNA, MicroRNA; NTA, Nanoparticle tracking analysis; PBS, Phosphate buffered saline; PFA, Paraformaldehyde; PMVECs, Pulmonary microvascular endothelial cells; RT-qPCR, Quantitative real-time PCR; Sema7A, Semaphorin 7A; TEM, Transmission electron microscopy; W/D, Wet-to-dry weight ratio.

Data Sharing Statement

The datasets generated and analyzed during the current study are available from the corresponding author on reasonable request.

Ethics Approval and Consent to Participate

All animal experiments were conducted under the rules approved by the Animal Care and Use Committee of Tianjin Nankai Hospital (Approval No. NKYY-DWLL-2022–031).

Acknowledgments

We thank all members of Tianjin key Laboratory of Acute Abdomen Disease Associated Organ Injury and ITCWM Repair, Institute of Acute Abdominal Diseases for providing a reliable platform and support for scientific research. We also appreciate Figdraw (www.figdraw.com) for assistance in animal and cells (Figure 1A and 1C) schematic templates. Additionally, we are grateful to editeg for their assistance in language polishing.

Author Contributions

All authors made a significant contribution to the work reported, whether that is in the conception, study design, execution, acquisition of data, analysis and interpretation, or in all these areas; took part in drafting, revising or critically reviewing the article; gave final approval of the version to be published; have agreed on the journal to which the article has been submitted; and agree to be accountable for all aspects of the work.

Funding

This study was supported by the National Natural Science Foundation of China (No. 82172121, No. 82372154).

Disclosure

The author(s) report no conflicts of interest in this work.

References

1. Singer M, Deutschman CS, Seymour CW. et al. The third international consensus definitions for sepsis and septic shock (Sepsis-3). *JAMA*. 2016;315(8):801–810. doi:10.1001/jama.2016.0287
2. Zhang J, Muri J, Fitzgerald G, et al. Endothelial lactate controls muscle regeneration from ischemia by inducing M2-like macrophage polarization. *Cell Metab*. 2020;31(6):1136–53.E7. doi:10.1016/j.cmet.2020.05.004
3. Wang Z, Wang Z. Park7 interacts with p47phox to direct NADPH oxidase-dependent ROS production and protect against sepsis. *Front Immunol*. 2023;14:1209438. doi:10.3389/fimmu.2023.1209438
4. Lin F-Y, Song C, Zeng Y-J, et al. Canagliflozin alleviates LPS-induced acute lung injury by modulating alveolar macrophage polarization. *Int Immunopharmacol*. 2020;88:106969. doi:10.1016/j.intimp.2020.106969
5. Vassiliou AG, Kotanidou A, Dimopoulou I, Orfanos SE. Endothelial damage in acute respiratory distress syndrome. *Int J mol Sci*. 2020;21 (22):8793. doi:10.3390/ijms21228793
6. Komarova YA, Kruse K, Mehta D, Malik AB. Protein interactions at endothelial junctions and signaling mechanisms regulating endothelial permeability. *Circ Res*. 2017;120(1):179–206. doi:10.1161/circresaha.116.306534
7. Al-Soudi A, Kaaij MH, Tas SW. Endothelial cells: from innocent bystanders to active participants in immune responses. *Autoimmun Rev*. 2017;16 (9):951–962. doi:10.1016/j.autrev.2017.07.008
8. Rotoli BM, Barilli A, Visigalli R, Ferrari F, Dall'Asta V. Endothelial cell activation by SARS-CoV-2 spike S1 protein: a crosstalk between endothelium and innate immune cells. *Biomedicines*. 2021;9(9):1220. doi:10.3390/biomedicines9091220
9. Nova Z, Skovierova H, Calkovska A. Alveolar-capillary membrane-related pulmonary cells as a target in endotoxin-induced acute lung injury. *Int J mol Sci*. 2019;20(4):831. doi:10.3390/ijms20040831
10. Wang R-J, Song W-L, Xie C-Y, et al. Urinary trypsin inhibitor protects tight junctions of septic pulmonary capillary endothelial cells by regulating the functions of macrophages. *J Inflamm Res*. 2021;14:1973–1989. doi:10.2147/jir.s303577
11. Sun W-F, Wu W-X, Jiang N, et al. Highly pathogenic PRRSV-infected alveolar macrophages impair the function of pulmonary microvascular endothelial cells. *Viruses*. 2022;14(3):452. doi:10.3390/v14030452
12. Birnhuber A, Fliesser E, Gorkiewicz G, et al. Between inflammation and thrombosis: endothelial cells in COVID-19. *Eur Respir J*. 2021;58 (3):2100377. doi:10.1183/13993003.00377-2021
13. Lai JJ, Chau ZL, Chen S-Y, et al. Exosome processing and characterization approaches for research and technology development. *Adv Sci*. 2022;9:2103222. doi:10.1002/advs.202103222
14. He C-J, Zheng S, Luo Y, Wang B. Exosome theranostics: biology and translational medicine. *Theranostics*. 2018;8(1):237–255. doi:10.7150/thno.21945
15. Feng Y, Bao X, Zhao J, Kang L, Sun X, Xu B. MSC-derived exosomes mitigate myocardial ischemia/reperfusion injury by reducing neutrophil infiltration and the formation of neutrophil extracellular traps. *Int J Nanomed*. 2024;19:2071–2090. doi:10.2147/IJN.S436925
16. El Andaloussi S, Mäger I, Breakefield XO, Wood MJA. Extracellular vesicles: biology and emerging therapeutic opportunities. *Nat Rev Drug Discov*. 2013;12(5):347–357. doi:10.1038/nrd3978
17. Zhang J, Li S, Li L, et al. Exosome and exosomal microRNA: trafficking, sorting, and function. *Genom Proteom Bioinf*. 2015;13:17–24. doi:10.1016/j.gpb.2015.02.001
18. Isaac R, Reis FCG, Ying W, Olefsky JM. Exosomes as mediators of intercellular crosstalk in metabolism. *Cell Metab*. 2021;33(9):1744–1762. doi:10.1016/j.cmet.2021.08.006
19. Xu N, Cui G, Zhao S, et al. Therapeutic effects of mechanical stress-induced C2C12-derived exosomes on glucocorticoid-induced osteoporosis through miR-92a-3p/PTEN/AKT signaling pathway. *Int J Nanomed*. 2023;18:7583–7603. doi:10.2147/IJN.S435301

20. Garcia-Martin R, Wang G-X, Brandão BB, et al. MicroRNA sequence codes for small extracellular vesicle release and cellular retention. *Nature*. 2022;601(7893):446–451. doi:10.1038/s41586-021-04234-3
21. An R, Li D, Dong -Y-Y, et al. Methylcobalamin protects melanocytes from H2O2-induced oxidative stress by activating the Nrf2/HO-1 pathway. *Drug Des Dev Ther*. 2021;15:4837–4848. doi:10.2147/DDDT.S336066
22. Zhang R-G, Pan K, Hao Y, Yip C-Y, Ko W-H. Anti-inflammatory action of HO-1/CO in human bronchial epithelium in response to cationic polypeptide challenge. *Mol Immunol*. 2019;105:205–212. doi:10.1016/j.molimm.2018.12.002
23. Dang X-M, He -B-B, Ning Q, et al. Alantolactone suppresses inflammation, apoptosis and oxidative stress in cigarette smoke-induced human bronchial epithelial cells through activation of Nrf2/HO-1 and inhibition of the NF-κB pathways. *Resp Res*. 2020;21:1–11. doi:10.1186/s12931-020-01358-4
24. Sha W-J, Zhao B, Wei H-Z, et al. Astragalus polysaccharide ameliorates vascular endothelial dysfunction by stimulating macrophage M2 polarization via potentiating Nrf2/HO-1 signaling pathway. *Phytomedicine*. 2023;112:154667. doi:10.1016/j.phymed.2023.154667
25. Shi J, Yu T-X, Song K, et al. Dexmedetomidine ameliorates endotoxin-induced acute lung injury in vivo and in vitro by preserving mitochondrial dynamic equilibrium through the HIF-1a/HO-1 signaling pathway. *Redox Biol*. 2021;41:101954. doi:10.1016/j.redox.2021.101954
26. Li X-Y, Yu J-B, Gong L-R, et al. Heme oxygenase-1 (HO-1) regulates Golgi stress and attenuates endotoxin-induced acute lung injury through hypoxia inducible factor-1α (HIF-1α)/HO-1 signaling pathway. *Free Radical Bio Med*. 2021;165:243–253. doi:10.1016/j.freeradbiomed.2021.01.028
27. Shi J, Yu JB, Zhang Y, et al. PI3K/Akt pathway - mediated HO - 1 induction regulates mitochondrial quality control and attenuates endotoxin - induced acute lung injury. *Lab Invest*. 2019;99(1795):–809. doi:10.1038/s41374-019-0286-x
28. Wu XY, Wu LL, Wu Y, et al. Heme oxygenase - 1 ameliorates endotoxin - induced acute lung injury by modulating macrophage polarization via inhibiting TXNIP/NLRP3 inflammasome activation. *Free Radical Bio Med*. 2023;194(12):22. doi:10.1016/j.freeradbiomed.2022.11.032
29. Dong S, Liu SS, Gao QY, et al. Interleukin - 17D produced by alveolar epithelial type II cells alleviates LPS - induced acute lung injury via the Nrf2 pathway. *Clin Sci*. 2023;137(1499):–512. doi:10.1042/CS20230354
30. Welsh JA, Goberdhan DCI, O'Driscoll L, et al. Minimal information for studies of extracellular vesicles (MISEV2023): from basic to advanced approaches. *J Extracell Vesicles*. 2024:13:e12404. 10.1002/jev2.12404.
31. Wang X, Xia J, Yang L, Dai J, He L. Recent progress in exosome research: isolation, characterization and clinical applications. *Cancer Gene Ther*. 2023;30(8):1051–1065. doi:10.1038/s41417-023-00617-y
32. Bao C, Xiang H, Chen Q, et al. A review of labeling approaches used in small extracellular vesicles tracing and imaging. *Int J Nanomed*. 2023;18:4567–4588. doi:10.2147/IJN.S416131
33. Middleton EA, Rowley JW, Campbell RA, et al. Sepsis alters the transcriptional and translational landscape of human and murine platelets. *Blood*. 2019;134(12):911–923. doi:10.1182/blood.2019000067
34. Zhang YD, Miao YY, Xiong XY, et al. Microglial exosomes alleviate intermittent hypoxia - induced cognitive deficits by suppressing NLRP3 inflammasome. *Biol Direct*. 2023;18(1):29. doi:10.1186/s13062-023-00387-5
35. Yue C, Wang W, Gao S, et al. Agomir miRNA-150-5p alleviates pristane-induced lupus by suppressing myeloid dendritic cells activation and inflammation via TREM-1 axis. *Inflamm Res*. 2023;72(7):1391–1408. doi:10.1007/s00011-023-01754-8
36. Qian Y, Chu G, Zhang L, et al. M2 macrophage-derived exosomal miR-26b-5p regulates macrophage polarization and chondrocyte hypertrophy by targeting TLR3 and COL10A1 to alleviate osteoarthritis. *J Nanobiotechnology*. 2024;22(1):72. doi:10.1186/s12951-024-02336-4
37. Xu X, Huang X, Xiao L, Wang J, Yang X, Wu Y. Mechanism of electro-acupuncture in alleviating intestinal injury in septic mice via polyamine-related M2-macrophage polarization. *Front Immunol*. 2024;15:1373876. doi:10.3389/fimmu.2024.1373876
38. Dumbuya JS, Li S, Liang L, Chen Y, Du J, Zeng Q. Effects of hydrogen-rich saline in neuroinflammation and mitochondrial dysfunction in rat model of sepsis-associated encephalopathy. *J Transl Med*. 2022;20(1):546. doi:10.1186/s12967-022-03746-4.
39. Jiao Y, Zhang T, Zhang CM, et al. Exosomal miR - 30d - 5p of neutrophils induces M1 macrophage polarization and primes macrophage pyroptosis in sepsis - related acute lung injury. *Crit Care*. 2021;25(1):–15. doi:10.1186/s13054-021-03775-3
40. Shi MM, Yang QY, Monsel A, et al. Preclinical efficacy and clinical safety of clinical-grade nebulized allogenic adipose mesenchymal stromal cells-derived extracellular vesicles. *J Extracell Vesicles*. 2021;10(e12134). doi:10.1002/jev2.12134
41. Dinh PUC, Paudel D, Brochu H, et al. Inhalation of lung spheroid cell secretome and exosomes promotes lung repair in pulmonary fibrosis. *Nat Commun*. 2020;11(1):1064. doi:10.1038/s41467-020-14344-7
42. Bosurgi L, Cao YG, Cabeza - Cabrerizo M, et al. Macrophage function in tissue repair and remodeling requires IL - 4 or IL - 13 with apoptotic cells. *Science*. 2017;356(1072):–6. doi:10.1126/science.aai8132
43. Shan X, Hu PH, Ni L, et al. Serine metabolism orchestrates macrophage polarization by regulating the IGF1–p38 axis. *Cell mol Immunol*. 2022;19(1263):–78. doi:10.1038/s41423-022-00925-7
44. Wang L, Y CAO, Gorshkov B, et al. Ablation of endothelial Pfkfb3 protects mice from acute lung injury in LPS - induced endotoxemia. *Pharmacol Res*. 2019;146:104292. doi:10.1016/j.phrs.2019.104292
45. Li K, Huang Z, Liu C, et al. Transcriptomic analysis of human pulmonary microvascular endothelial cells treated with LPS. *Cell Signal*. 2023;111:110870. doi:10.1016/j.cellsig.2023.110870
46. Huang CY, Wang J, Liu HB, et al. Ketone body β - hydroxybutyrate ameliorates colitis by promoting M2 macrophage polarization through the STAT6 - dependent signaling pathway. *Bmc Med*. 2022;20(1):148. doi:10.1186/s12916-022-02352-x
47. Gong LR, Kan YX, Lian Y, et al. Electroacupuncture attenuates limb ischemia - reperfusion - induced lung injury via p38 mitogen - activated protein kinase - nuclear factor erythroid - 2 - related factor - 2/heme oxygenase pathway. *J Surg Res*. 2020;246(170):–81. doi:10.1016/j.jss.2019.08.021
48. Yu JB, Shi J, Wang D, et al. Heme oxygenase - 1/carbon monoxide - regulated mitochondrial dynamic equilibrium contributes to the attenuation of endotoxin - induced acute lung injury in rats and in lipopolysaccharide - activated macrophages. *Anesthesiology*. 2016;125(1190):–201. doi:10.1097/aln.0000000000001333
49. Tian J, Li YN, Mao X, et al. Effects of the PI3K/Akt/HO - 1 pathway on autophagy in a sepsis - induced acute lung injury mouse model. *Int Immunopharmacol*. 2023;124:111063. doi:10.1016/j.intimp.2023.111063
50. Shutong L, Yu J, Jia W, et al. HO-1/autophagic flux axis alleviated sepsis-induced acute lung injury via inhibiting NLRP3 inflammasome. *Cell Signal*. 2022;100:110473. doi:10.1016/j.cellsig.2022.110473

51. Chen SY, Chen YL, Li PC, et al. Engineered extracellular vesicles carrying let - 7a - 5p for alleviating inflammation in acute lung injury. *J Biomed Sci*. 2024;31(1):30. doi:10.1186/s12929-024-01019-4
52. Shi MM, Yang QY, Monsel A, et al. Preclinical efficacy and clinical safety of clinical-grade nebulized allogenic adipose mesenchymal stromal cells-derived extracellular vesicles. *J Extracell Vesicles*. 2021;10(10):e12134. doi:10.1002/jev2.12134
53. Han YH, Zhu Y, Youngblood HA, et al. Nebuization of extracellular vesicles: a promising small RNA delivery approach for lung diseases. *J Control Release*. 2022;352(556):–69. doi:10.1016/j.jconrel.2022.10.052
54. Wang Z, Popowski KD, Zhu D, et al. Exosomes decorated with a recombinant SARS-CoV-2 receptor-binding domain as an inhalable COVID-19 vaccine. *Nat Biomed Eng*. 2022;6(7):791–805. doi:10.1038/s41551-022-00902-5
55. Yamashita M, Niisato M, Kawasaki Y, et al. VEGF - C/VEGFR - 3 signalling in macrophages ameliorates acute lung injury. *Eur Respir J*. 2022;59 (4):2100880. doi:10.1183/13993003.00880-2021
56. Carden D, Xiao F, Moak C, Willis BH, Robinson - jackson S, Alexander S. Neutrophil elastase promotes lung microvascular injury and proteolysis of endothelial cadherins. *Am J Physiol - Heart C*. 1998;275:H385–H92. doi:10.1152/ajpheart.1998.275.2.h385
57. Groeneveld ABJ. Vascular pharmacology of acute lung injury and acute respiratory distress syndrome. *Vasc Pharmacol*. 2002;39(247):–56. doi:10.1016/s1537-1891(03)00013-2
58. Laurent P, Lapoirie J, Leleu D, et al. Interleukin-1β-activated microvascular endothelial cells promote DC-SIGN-Positive alternatively activated macrophages as a mechanism of skin fibrosis in systemic sclerosis. *Arthritis Rheumatol*. 2022;74(1013):–26. doi:10.1002/art.42061
59. Wang D, Wang XH, Si MH, et al. Exosome - encapsulated miRNAs contribute to CXCL12/CXCR4 - induced liver metastasis of colorectal cancer by enhancing M2 polarization of macrophages. *Cancer Lett*. 2020;474(36):–52. doi:10.1016/j.canlet.2020.01.005
60. Gao L, Qiu F, Cao H, et al. Therapeutic delivery of microRNA - 125a - 5p oligonucleotides improves recovery from myocardial ischemia/ reperfusion injury in mice and swine. *Theranostics*. 2023;13(2):685–703. doi:10.7150/thno.73568
61. Zhou XQ, Hong YL, Liu YP, et al. Intervening in hnRNPA2B1 - mediated exosomal transfer of tumor - suppressive miR - 184 - 3p for tumor microenvironment regulation and cancer therapy. *J Nanobiotechnol*. 2023;21(1):422. doi:10.1186/s12951-023-02190-w
62. Guo XF, Qiu W, Wang CC, et al. Neuronal activity promotes glioma progression by inducing proneural - to - mesenchymal transition in glioma stem cells. *Cancer Res*. 2024;84(372):–87. doi:10.1158/0008-5472.can-23-0609
63. Lu QY, Liu ZT, Zhao LY, et al. Sema7A protects against high - fat diet - induced obesity and hepatic steatosis by regulating adipo/lipogenesis. *mol Metab*. 2023;70:101698. doi:10.1016/j.molmet.2023.101698
64. Song Y, Wang L, Zhang L, Huang DM. The involvement of semaphorin 7A in tumorigenic and immunoinflammatory regulation. *J Cell Physiol*. 2021;236(6235):–48. doi:10.1002/jcp.30340
65. Qi WN, Zeng D, Xiong XS, Hu Q. Knockdown of SEMA7A alleviates MPP+-induced apoptosis and inflammation in BV2 microglia via PPAR-γ activation and MAPK inactivation. *Immun Inflamm Dis*. 2023;11:e756. doi:10.1002/iid3.756